Plant Cell Reports
https://doi.org/10.1007/s00299-021-02771-9

ORIGINAL ARTICLE

RIN4 homologs from important crop species differentially regulate the *Arabidopsis* NB-LRR immune receptor, RPS2

Maheen Alam[1,2] · Jibran Tahir[3] · Anam Siddiqui[4] · Mazin Magzoub[5] · Syed Shahzad-ul-Hussan[1] · David Mackey[2,6] · A. J. Afzal[5]

Received: 7 April 2021 / Accepted: 9 August 2021

Abstract

Key message **RIN4 homologs from important crop species differ in their ability to prevent ectopic activity of the nucleotide binding-leucine rich repeat resistance protein, RPS2.**

Abstract Pathogens deploy virulence effectors to perturb host processes. Plants utilize intracellular resistance (R) proteins to recognize pathogen effectors either by direct interaction or indirectly via effector-mediated perturbations of host components. RPM1-INTERACTING PROTEIN4 (RIN4) is a plant immune regulator that mediates the indirect activation of multiple, independently evolved R-proteins by multiple, unrelated effector proteins. One of these, RPS2 (RESISTANT TO *P. SYRINGAE*2), is activated upon cleavage of *Arabidopsis* (At)RIN4 by the *Pseudomonas syringae* effector AvrRpt2. To gain insight into the AvrRpt2-RIN4-RPS2 defense-activation module, we compared the function of AtRIN4 with RIN4 homologs present in a diverse range of plant species. We selected seven homologs containing conserved features of AtRIN4, including two NOI (Nitrate induced) domains, each containing a predicted cleavage site for AvrRpt2, and a C-terminal palmitoylation site predicted to mediate membrane tethering of the proteins. Palmitoylation-mediated tethering of AtRIN4 to the plasma membrane and cleavage by AvrRpt2 are required for suppression and activation of RPS2, respectively. While all seven homologs are localized at the plasma membrane, only four suppress RPS2 when transiently expressed in *Nicotiana benthamiana*. All seven homologs are cleaved by AvrRpt2 and, for those homologs that are able to suppress RPS2, cleavage relieves suppression of RPS2. Further, we demonstrate that the membrane-tethered, C-terminal AvrRpt2-generated cleavage fragment is sufficient for the suppression of RPS2. Lastly, we show that the membrane localization of RPS2 is unaffected by its suppression or activation status.

Keywords RIN4 homologs · RPS2 · AvrRpt2 · R-protein · *Nicotiana benthamiana* · *Pseudomonas syringae*

Communicated by Eugenio Benvenuto.

✉ A. J. Afzal
aja11@nyu.edu

[1] Department of Biology, Lahore University of Management Sciences, Sector U, DHA, Lahore, Pakistan

[2] Department of Horticulture and Crop Science, The Ohio State University, Columbus, OH 43210, USA

[3] The New Zealand Institute for Plant and Food Research Limited, Private Bag 92-169, Auckland 1025, New Zealand

[4] Department of Plant Sciences, Rothamsted Research, West Common, Harpenden AL52JQ, UK

[5] Biology Program, New York University Abu Dhabi, Abu Dhabi, UAE

[6] Department of Molecular Genetics and Center for Applied Plant Sciences, The Ohio State University, Columbus, OH 43210, USA

Introduction

Plants have evolved a sophisticated innate immune system to defend themselves against invading pathogens. Although plants lack mobile immune cells, they have developed immune receptors that recognize pathogen molecules (Jones and Dangl 2006). Pathogen recognition by plant cells relies on membrane-localized and intracellular receptors (Bonardi et al. 2012; Macho and Zipfel 2015; Monteiro and Nishimura 2018). The former are typically activated by microbe-associated molecular patterns (MAMPs), such as lipopolysaccharides, flagellin or chitin, leading to MAMP triggered immunity (MTI) (Chisholm et al. 2006; Glowacki et al. 2011; Khan et al. 2016; Zipfel 2014). Most of the intracellular receptors, known as resistance (R) proteins, belong to the nucleotide binding and leucine rich repeat (NLRs) family

Published online: 05 September 2021

of receptors (Bonardi et al. 2012; Chiang and Coaker 2015; Chisholm et al. 2006; Monteiro and Nishimura 2018). Perception by NLRs, of effector proteins from potential pathogens, including the type three effectors (T3Es) translocated from gram negative bacteria into host cells, leads to effector triggered immunity (ETI) that frequently culminates in a hypersensitive response characterized by programmed cell death (PCD) (Chiang and Coaker 2015; Dodds and Rathjen 2010; Jones and Dangl 2006; Monteiro and Nishimura 2018).

NLRs can detect effector proteins either directly or indirectly. Many pathogens have been reported to possess hundreds of effector proteins (Jones and Dangl 2006); whereas plants have more limited allelic diversity at the R loci and these alleles are maintained by balancing selection (Bergelson et al. 2001; Van der Hoorn 2002). This excess of effectors relative to R-proteins, as well as selective pressure favoring effector variants that evade detection, limits the effectiveness of direct recognition of effectors. Indirect detection, which is based on perception of an effector-induced perturbation within a host cell, allows plants to use their limited repertoire of NLRs to detect a larger number of effectors, as the effectors converge on a finite set of host targets (Dangl and McDowell 2006). Because indirect recognition is often triggered by perturbations resulting from the virulence activity of effectors, effectors are constrained in their ability to retain function while evading detection.

A well-characterized example of a host protein that mediates indirect recognition of effectors is RPM1 interacting protein 4 (RIN4). AtRIN4 is a small, intrinsically unstructured protein that contains two NOI (Nitrate induced) domains (with no known biochemical function) and is localized at the plasma membrane because of the palmitoylation of its C-terminal cysteine residues (Afzal et al. 2013; Day et al. 2005; Desveaux et al. 2007; Takemoto and Jones 2005; Toruno et al. 2019). The AtRIN4 protein is targeted by five unrelated *Pseudomonas syringae* effectors, AvrRpm1, AvrB, AvrRpt2, HopF2 and HopZ3 (Lee et al. 2015; Mackey et al. 2002, 2003; Redditt et al. 2019; Wilton et al. 2010). In the absence of effector-targeting, RIN4 negatively regulates MTI (Kim et al. 2005b). The effectors that target RIN4 promote virulence, at least in part, by enhancing its negative regulation of MTI. For example, AvrRpt2 is a cysteine protease that cleaves AtRIN4 at conserved motifs, VPXFGXW, present at the N-terminal side of both NOI domains (Axtell and Staskawicz 2003; Chisholm et al. 2005; Kim et al. 2005a; Takemoto and Jones 2005). Two of the resulting fragments, termed AvrRpt2-cleavage product 2 (ACP2, AtRIN4$^{11-152}$) and ACP3 (AtRIN4$^{153-211}$) are hyperactive suppressors of MTI, relative to full length AtRIN4 (Afzal et al. 2011). AtRIN4 associates with two plasma-membrane localized NLRs, RPM1 and RPS2, and its perturbation by AvrRpm1, AvrB, or AvrRpt2 elicits their partial or full activation (Axtell and Staskawicz 2003; Chung et al. 2011; Day et al. 2005; Kim et al. 2009; Mackey et al. 2002, 2003). These findings establish AtRIN4 as a hub at the nexus of MTI, effector-induced suppression of MTI, and effector-induced activation of ETI in *Arabidopsis*.

RIN4 homologs with N-terminal and C-terminal NOI domains and a putative C-terminal palmitoylation site exist in a wide variety of plant species, including mosses, monocots and dicots (Afzal et al. 2013). Several of these RIN4 homologs, including those from lettuce (*Lactuca sativa*), tomato (*Solanum lycopersicum*), soybean (*Glycine max*), barley (*Hordeum vulgare*) and apple (*Malus domestica*), regulate plant immunity (Gill et al. 2012; Jeuken et al. 2009; Luo et al. 2009; Mazo-Molina et al. 2020; Prokchorchik et al. 2020; Selote and Kachroo 2010b). Soybean contains four RIN4 homologs, each of which contains a putative C-terminal palmitoylation site and are plasma membrane localized (Selote and Kachroo 2010b). Similar to AtRIN4, GmRIN4a and GmRIN4b negatively regulate basal immunity; silencing of either homolog resulted in enhanced resistance to virulent strains of *P. syringae* (Selote and Kachroo 2010a, b). Also similar to AtRIN4, GmRIN4a and GmRIN4b are targeted by the effectors AvrB, AvrRpm1 and AvrRpt2, possibly to enhance negative regulation of MTI (Ashfield et al. 2014; Selote and Kachroo 2010b). However, unlike the recognition of AvrB or AvrRpm1 by a single R-protein (RPM1) in *Arabidopsis*, AvrB and AvrRpm1 are recognized in resistant soybean cultivars by two independently evolved R-proteins, Rpg1b and Rpg1r, respectively (Ashfield et al. 2014; Selote and Kachroo 2010b). Although AvrRpt2 elicits an effective defense response on some soybean cultivars (Whalen et al. 1991), the relationship of GmRIN4 homologs to RPS2 is unknown. More recently, it has been demonstrated that AvrRpt2-mediated cleavage of SlRIN4 and MdRIN4 results in the activation of two independently evolved NLR-proteins, Ptr1 in tomato and Mr5 in apple (Mazo-Molina et al. 2020; Prokchorchik et al. 2020). AtRIN4 prevents ectopic activation, defined as that occurring in the absence of effector-activation, of RPS2 in unchallenged *Arabidopsis* and *N. benthamiana* plants (Day et al. 2005; Mackey et al. 2003). By contrast, MR5 is not ectopically active, but ACP3 is sufficient to activate it (Prokchorchik et al. 2020). Collectively, these findings indicate that a variety of NLR-proteins distinctly monitor the status of RIN4. Conservation of RIN4 in crop species leads to the hypothesis that those RIN4 homologs are able to regulate the activity of RPS2. Since AvrRpt2-like effectors with the capacity to specifically cleave RIN4 are found in a diverse collection of plant pathogens (Eschen-Lippold et al. 2016; Mazo-Molina et al. 2020; Prokchorchik et al. 2020), understanding the ability of RIN4 homologs to function with RPS2 could enable the development of crops resistant to a variety of pathogens.

In this study, we show that, similar to AtRIN4, RIN4 homologs from seven crop species all localize at the plasma membrane. Despite this common localization, the RIN4 homologs differ in their ability to suppress RPS2. We also demonstrate that all RIN4 homologs are cleaved by AvrRpt2 and, for those capable of suppressing RPS2, this cleavage results in RPS2 activation. Surprisingly, the central ($RIN4^{INT}$) and C-terminal ($RIN4^{CLV3}$) fragments of RIN4 generated upon AvrRpt2-cleavage differ in their regulation of RPS2. The membrane-tethered $RIN4^{CLV3}$ fragments, comparable to ACP3, suppress RPS2 activation. The non-membrane-tethered $RIN4^{INT}$ fragments, comparable to ACP2 fail to suppress RPS2. Lastly, we demonstrate that the plasma membrane localization of RPS2 is unaffected by its suppression/activation status.

Methods

Plants and growth conditions

For *Agrobacterium* infiltrations, *Nicotiana benthamiana* seeds were sown in soil (Peat moss, Pindstrup færdigblanding substrate) and grown at 24 °C (day) and 22 °C (night) in a growth chamber under an 8-h light/16-h dark cycle. After 2 weeks of germination, seedlings were transferred to pots (one seedling per pot). The seedlings were further grown for 4 weeks after which they were ready for *Agrobacterium* infiltrations. Fully expanded *N. benthamiana* leaves were used to carry out bacterial infiltrations. To prepare RNA, *Arabidopsis thaliana* (Col-0), *Lactuca sativa* (Lettuce), *Oryza sativa* (Rice), *Malus domestica* (Apple), *Solanum lycopersicum* (tomato), *Solanum tuberosum* (potato), *Prunus persica* (peach), and *Glycine max* (soybean) seeds were also sown in soil (Peat moss, Pindstrup færdigblanding substrate) and grown at 24 °C (day) and 22 °C (night) in a growth chamber under an 8-h light/16-h dark cycle. Leaves were harvested from 4-week-old plants and were stored in a –80 °C freezer.

Plasmid construction

The homologous RIN4 constructs were cloned using the Gateway system (Invitrogen, Carlsbad, CA). To prepare RNA, the harvested leaves were ground by mortar and pestle in liquid nitrogen. RNA was extracted using Trizol following the manufacturer's protocol (Invitrogen, Carlsbad, CA). The corresponding cDNAs were synthesized using M-MLV Reverse transcriptase following the manufacturer's protocol (Invitrogen Carlsbad, CA). Using cDNA as template, RIN4 homologs were amplified through polymerase chain reaction (PCR). All primers, used for the purpose of cloning, were designed in such a way that they incorporated a CACC tag at the 5' end of each construct (Supplemental Table 1). Primers used for the amplification of homologous $RIN4^{1\Delta RCS1}$ and $RIN4^{INT}$ (Internal) equivalent fragments were specifically designed to introduce an AcV5 tag at the 5' end of each construct and to exclude the region corresponding to the first 12 or 13 amino acids or 1ΔRCS1 (RIN4 cleavage site 1). Sequence data from this study can be found in the accession numbers mentioned in Supplemental Table 1.

Phusion® DNA Polymerase (NEB, Ipswich, MA) was used for the gene-specific amplification of the homologous RIN4 constructs and RPS2. PCR amplified genes were cloned into the entry vector, pENTR™ Directional TOPO (D-TOPO) (Invitrogen, Carlsbad, CA). The gateway binary vector pEarley Gate 104 (35S promoter, YFP:N) was used as the destination vector for the homologous RIN4 derivatives; while pEarley Gate 101 (35S promoter, C:YFP-HA) was used as the destination vector for RPS2. Since the entry and the destination vector had the same antibiotic selection marker (Kanamycin), we followed the PCR amplification based (PAB) method to mobilize the inserts from the entry clones to the destination vector (Kumar et al. 2013). The insert was amplified from the entry vector using M13 primers (Supplemental Table 1) and was subsequently cloned into the destination vector using LR Clonase™ (Invitrogen Carlsbad, CA). The destination vector was then transformed in *A. tumefaciens* GV3101 pMP90 cells. AtRIN4 derivative, $RIN4^{11-211}$ was amplified using primers that added an AcV5 tag and a sequence that encodes a 15 amino acid linker (NELALKAAGADINKT) at the 5' end of the insert. The chimeric insert was cloned into pENTR-D-TOPO and subsequently moved into the gateway binary vector pB2GW7 (containing a 35S promoter).

A. tumefaciens strain C58-C1 carrying RPS2-HA, expressed under the control of a promoter (pOCS:RPS2-HA), was a gift from Dr. Brad Day and has been described previously (Day et al. 2005). AvrRpt2-HA and $AvrRpt2^{C122A}$-HA, expressed under the control of a 35S promoter, were a gift from Dr. Kee Hoon Sohn and have been described previously (Prokchorchik et al. 2020). p19 (silencing suppressor) expressed under the control of a 35S promoter has been described previously (Hamilton et al. 2002; Prado et al. 2019). RFP-OsRac1 expressed under the control of 35S promoter (pGDR vector backbone) was a gift from Dr. Guo-Liang Wang. RFP fused OsRac1, a GTPase, has been used as a plasma membrane marker previously (Fan et al. 2018).

Agrobacterium-mediated transient expression

A. tumefaciens strains carrying the homologous 35S:YFP-AcV5-RIN4 derivatives, pOCS:RPS2-HA or 35S:RPS2-YFP-HA, 35S:AvrRpt2-HA or 35S:$AvrRpt2^{C122A}$-HA were grown overnight at 28 °C in Luria Bertani (LB) media containing the appropriate antibiotics (100 µg/ml of kanamycin,

50 µg/ml of gentamycin, 100 µg/ml of rifampicin or 5 µg/ml of tetracycline). The overnight cultures were centrifuged at 4500 × g for 10 min. The pellet collected was re-suspended in induction media (10 mM MES pH5.6, 10 mM $MgCl_2$ and 200 µM acetosyringone). The OD_{600} (optical density) of the cultures, as required for each assay, was adjusted using the induction media. For all infiltrations, the final OD_{600} of *A. tumefaciens* strains carrying the desired construct(s), was adjusted to a constant total OD_{600} using *A. tumefaciens* strain GV3101. *A. tumefaciens* strain(s) were infiltrated into *N. benthamiana* leaves as described previously (Day et al. 2005; Tai et al. 1999).

Confocal microscopy analysis

The localization of homologous YFP-AcV5-RIN4 derivatives and RPS2-YFP-HA was observed at the indicated time points. Leaf discs from the infiltrated area were obtained and the YFP signal was observed using a confocal microscope (Nikon Eclipse Ti/C2/C2Si) (Nikon, Foster City, CA) using an excitation wavelength of 514 nm and an emission wavelength of 530 nm. Nuclei in the infiltrated region, were stained by infiltrating 1 µg/ml DAPI D3571 dye (Invitrogen, Eugene, OR) into *N. benthamiana* leaves, 6 h before imaging. The fluorescence from the DAPI stained nuclei was observed using an excitation wavelength of 358 nm and an emission wavelength of 461 nm. Co-localization of YFP-RIN4 derivatives and RFP-OsRac1 was observed at the indicated time points. RFP signal was observed using an excitation wavelength of 561 nm and an emission wavelength of 575 nm.

Protein extraction and SDS-PAGE

To determine expression of the transiently expressed YFP-AcV5-RIN4 derivatives, total protein was extracted from the plant tissue as described previously (Afzal et al. 2011). Briefly, 0.1 g (g) leaf tissue was homogenized in 300 µl of extraction buffer, 20 mM Tris, 150 mM NaCl, 1 mM EDTA, 1% TritonX-100, 0.1% SDS, 5 mM DTT and 10X plant protease inhibitor cocktail (Sigma-Aldrich, Saint Louis, MO). The samples were centrifuged at 13,523×*g* for 20 min at 4 °C to remove the insoluble debris. To 100 µl of the collected supernatant (total protein), 5X SDS-PAGE loading dye was added, and the samples were heated at 65 °C for 10 min. The protein samples were resolved on 12% (w/v) SDS-PAGE gels and were subsequently transferred to nitrocellulose membrane. The membrane was probed with 1:5000 dilution of anti-GFP antibody (Abcam, Cambridge, UK) to detect YFP-tagged RIN4 derivatives. For protein detection, the blot was probed with ECL following manufacturer's protocol (GE Healthcare Amersham, Buckinghamshire, UK) and chemiluminescence was observed using the ChemiDoc XRS system (Bio-Rad, Hercules, CA).

Subcellular fractionation

To separate membrane proteins from soluble proteins, 0.1 g leaf tissue was ground in liquid nitrogen and resuspended in 700 µl of homogenization buffer (30 mM Tris PH 8.3, 150 mM NaCl, 1 mM EDTA, 20% glycerol, 5 mM DTT, 10X protease inhibitor and 10 mM PMSF). The samples were centrifuged at 13,523×g for 10 min at 4 °C to remove insoluble debris. The "total" fraction consisted of the supernatant from this first spin combined directly with the SDS-PAGE loading dye and heated at 65 °C for 10 min. For fractionation of the microsomal fraction, 600 µl of supernatant from the first spin was combined with 20 µl of 1 M $CaCl_2$ and incubated on ice for 90 min prior to centrifugation at 21,130×*g* for 90 min at 4 °C. The "soluble" fraction (supernatant from the second spin) was combined with the loading dye and heated at 65 °C for 10 min. The pellet from the second spin was re-suspended in 100 µl of resuspension buffer (10 mM Tris pH 7.6, 150 mM NaCl, 0.1 mM EDTA, 10% glycerol, 10X protease inhibitor, 10 mM PMSF) and centrifuged again at 21,130×*g* for 60 min at 4 °C. The "microsomal membrane" fraction (the final pellet) was resuspended in 90 µl of 1X SDS-PAGE loading dye and heated at 65 °C for 15 min. The subcellular fractions were resolved on either 12% (w/v) SDS-PAGE or 4–20% (w/v) precast TGX (Bio-Rad, Hercules, CA) gels and were subsequently transferred to nitrocellulose membrane. The membrane was probed with 1:5000 dilution of anti-GFP antibody (Abcam, Cambridge, UK) to detect YFP-tagged RIN4 derivatives. A 1:600 dilution of H^+-ATPase (Agrisera, Vannas, SE) was used as a plasma membrane marker.

Quantification of hypersensitive response

To quantify the Hypersensitive Response, ion leakage from leaf discs corresponding to the agro-infiltrated area of *N. benthamiana* leaves was measured. Leaf discs were submerged in 15 ml of water and cell death was quantified at the indicated time points with the aid of a conductivity meter (WTW, Weilheim, Germany). For each construct, ion leakage data were generated from three to five biological replicates (three technical replicates per biological replicate). Background correction was based on the conductivity from leaf discs corresponding to un-infiltrated *N. benthamiana* leaves. Cell death in intact leaves was detected by observing

leaf autofluorescence using the ChemiDoc XRS Imager (Bio-Rad, Hercules, CA).

Protein alignment

The homologous RIN4 protein sequences were aligned by ClustalW using MEGA-X. Alignments were generated with a reduced Gap penalty (4.0) for both pairwise and multiple sequence alignments. Pairwise sequence similarity and identity for the multiple sequence alignments was calculated by the BLOSUM 62 scoring Matrix with the SIAS (sequence identity and similarity) tool.

Palmitoylation prediction

Putative palmitoylation residues in the homologous RIN4 sequences were predicted using CSS-Palm 4.0 (Zhou et al. 2006) with the threshold stringency set to medium (http://csspalm.biocuckoo.org). The software employs a clustering and scoring strategy algorithm (CSS), a group-based prediction system (GPS) as well as a training dataset that comprises 277 proteins that contain 583 palmitoylation sites to accurately predict putative palmitoylation sites in query proteins (Ren et al. 2008; Weng et al. 2017).

Results

RIN4 homologs are present in important crop species

While RIN4 homologs are present in plant species dating as far back as moss, only a few of them have been reported to regulate innate immunity in their respective host species (Afzal et al. 2013; Jeuken et al. 2009; Mazo-Molina et al. 2020; Prokchorchik et al. 2020; Selote and Kachroo 2010b). We initially performed protein blast using AtRIN4 as a query to identify seven RIN4 homologs in notable annual and perennial crop plants including *G. max* (soybean, GmRIN4), *L. sativa* (lettuce, LsRIN4), *M. domestica* (apple, MdRIN4) *O. sativa* (rice, OsRIN4), *P. persica* (peach, PpRIN4), *S. lycopersicum* (tomato, SlRIN4) and *S. tuberosum* (potato, StRIN4). The regions of AtRIN4 known to participate in immune regulation (Fig. 1a), including the N-NOI and C-NOI domains present at the N- and C-terminal regions of the proteins, respectively (Afzal et al. 2011; Day et al. 2005), were well conserved in the homologous proteins (Fig. 1b, Supplemental Table 2). The C-NOI domains of the homologs show greater sequence conservation relative to the N-NOI domain, consistent with previously published data (Supplemental Table 2) (Afzal et al. 2013). The N-terminal portion of both NOI domains within the homologs also contains a consensus AvrRpt2 cleavage site (RCS: VPXFGXW, Supplemental Table 2). Lastly, each homolog also contains two or three cysteine residues near its C-terminus, within a predicted palmitoylation target site (Supplemental Table 3) that is crucial for membrane localization of AtRIN4 (Day et al. 2005; Kim et al. 2005a; Takemoto and Jones 2005).

RIN4 homologs localize at the plasma membrane

Based on the putative palmitoylation target sites, we predicted that, like AtRIN4, the RIN4 homologs would also localize at the plasma membrane. To test their membrane localization, derivatives lacking the first 12 or 13 amino acids and containing instead an N-terminal YFP- and AcV5-tag were constructed (YFP-AcV5-RIN4$^{1\Delta RCS1}$; for the structure of this and all protein derivatives used in this study, see Supplemental Fig. 1). When expressed in *N. benthamiana* using *Agrobacterium*-mediated infiltrations, fluorescent microscopy indicated that these derivatives all localized to the cell periphery, consistent with the predicted plasma membrane localization and in contrast to free YFP protein, which localized to the cytosol and the nucleus (Fig. 2a). Furthermore the YFP-RIN4 derivatives colocalilzed with RFP fused OsRac1, a small plasma membrane GTPase (Supplemental Fig. 2a). Subcellular fractionation confirmed that, similar to AtRIN4, all the YFP-tagged derivatives of the RIN4 homologs accumulated in the microsomal membrane fraction while free YFP protein accumulated in the soluble fraction (Fig. 2b and Supplemental Fig. 2b). Together, these observations indicate that, like AtRIN4, the homologs under study all localize to the plasma membrane.

RIN4 homologs differ in their ability to suppress RPS2

Plasma membrane localization of AtRIN4 is crucial for the suppression of RPS2-induced cell death in *N. benthamiana* and *Arabidopsis* (Afzal et al. 2011; Day et al. 2005). Despite the shared localization of all of the RIN4 homologs, only a subset were able to suppress RPS2 when co-expressed transiently in *N. benthamiana* (Fig. 3a, b). The ability of full-length (Fl) AtRIN4 to suppress RPS2 was matched by YFP-AcV5-AtRIN4$^{1\Delta RCS1}$ (Supplemental Fig. 3) and, similar to YFP-AcV5-AtRIN4$^{1\Delta RCS1}$, the YFP-AcV5-RIN4$^{1\Delta RCS1}$ versions from soybean, peach, potato and apple also suppressed RPS2 (Fig. 3a, b and supplemental Fig. 4). In contrast, the

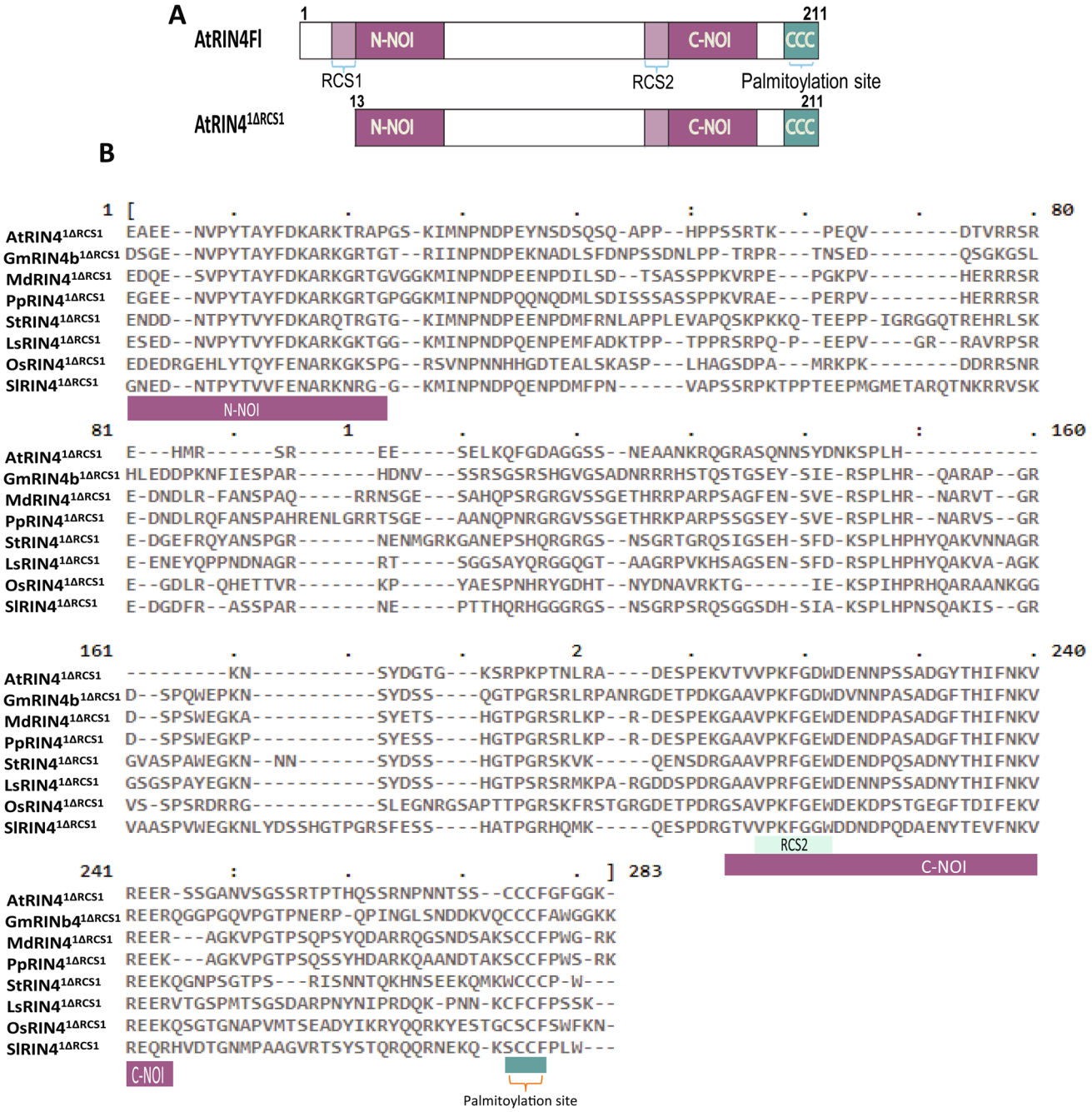

Fig. 1 In silico analysis of RIN4 homologs from important crop plants. **A** Schematic representations of wild-type AtRIN4 and its 1ΔRCS1 derivative. Indicated are the NOI (Nitrate induced) domains of unknown function, the AvrRpt2-cleavage sites (RCS1 & RCS2) present at the N-terminal side of the NOI domains, and the C-terminal palmitoylation motif with targeted cysteine residues (shown in green). **B** Alignment of the amino acid sequence of AtRIN4$^{1\Delta RCS1}$ and 1ΔRCS1 derivatives of homologs from various plant species, Arabidopsis (At), Soybean (Gm), Peach (Pp), Potato (St), Lettuce (Ls), Rice (Os) and Tomato (St). Indicated are conserved domains, including the N-NOI, RCS2/C-NOI domains, and the C-terminal cysteine residues predicted to serve as sites for palmitoylation

YFP-AcV5-RIN4$^{1\Delta RCS1}$ versions from lettuce, rice and tomato failed to suppress RPS2. The differences in RPS2-suppression were unlikely due to insufficient expression of the RIN4 derivatives relative to RPS2 because the same pattern was observed when RPS2 was expressed to lower or higher levels through the use of different titers of *Agrobacterium* (Supplemental Figs. 4 and 5). Also, the ability of the derivatives to suppress RPS2 did not correlate with their expression level (Fig. 3c). Taken together, these results indicate that plasma membrane-localized homologs of RIN4

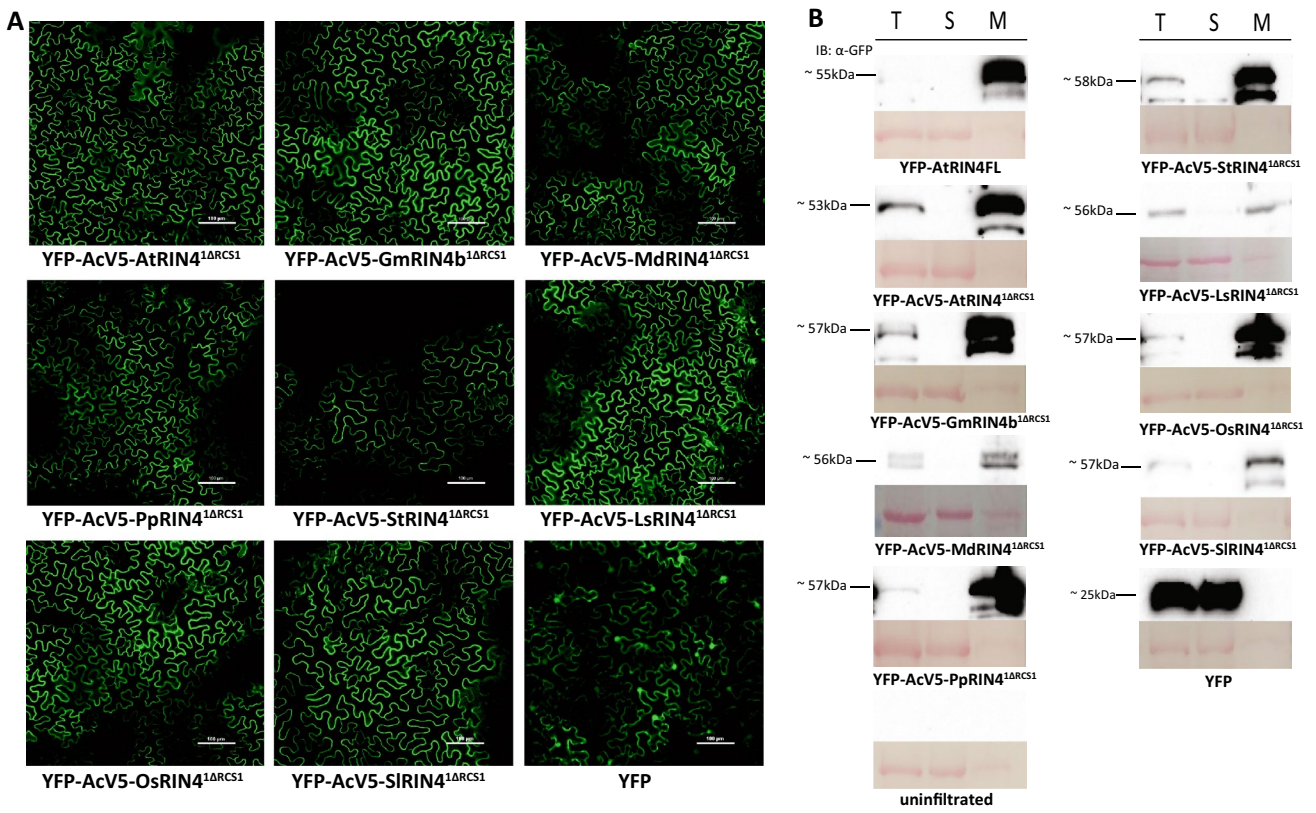

Fig. 2 RIN4 homologs localize at the plasma membrane. Homologous YFP-AcV5-RIN4$^{1\Delta RCS1}$ derivatives (OD_{600} 1.0) were transiently expressed in *N. benthamiana* plants. **A** Fluorescent signal was observed at 72 h post infiltration (HPI) using confocal microscopy (Scale bar: 100 µM). All RIN4 homologs localized at the membrane, while free YFP protein localized in the cytosol and the nucleus. Arabidopsis (At), Soybean (Gm), Peach (Pp), Potato (St), Lettuce (Ls), Rice (Os) and Tomato (St). **B** Anti-GFP immunoblotting was conducted on samples at 72 HPI. The samples were fractionated into total (T), soluble (S) and membrane (M) fractions. YFP-AcV5-RIN4$^{1\Delta RCS1}$ homologs accumulated in the membrane fraction, while the free YFP protein accumulated in the soluble fraction. Panels below show ponceau stain of RuBisCO as a soluble protein marker. IB, immunoblot. Molecular masses indicate the predicted mobility of the protein(s) of interest

homologs can be divided into two groups based on their ability to suppress RPS2.

AvrRpt2-mediated cleavage of YFP-AcV5-RIN4$^{1\Delta RCS1}$ derivatives generates soluble and membrane-tethered cleavage products

AvrRpt2 is a cysteine protease that, by cleaving at VPXF-GXW target sites at the N-terminal side of both NOI domains within AtRIN4, generates three fragments: RIN4$^{1-10}$ (ACP1 or CLV1), RIN4$^{11-152}$ (ACP2 or CLV2), and RIN4$^{153-211}$ (ACP3 or CLV3), (Fig. 1a and Supplemental Fig. 1) (Afzal et al. 2011; Chisholm et al. 2005; Kim et al. 2005a; Takemoto and Jones 2005). AvrRpt2 cleavage sites are conserved in RIN4 homologs in a wide variety of plant species (Afzal et al. 2013; Sun et al. 2014). More recently it has been demonstrated that AvrRpt2 from *P. syringae* and *Erwinia amylovora*, when expressed in *N. benthamiana*, cleaves SlRIN4 and MdRIN4, respectively (Mazo-Molina et al. 2020; Prokchorchik et al. 2020). Thus, the conserved target site within RIN4 from distantly related plant species is cleaved by AvrRpt2 effectors from diverse bacterial pathogens. Since they contain the AvrRpt2 cleavage sites, we hypothesized that the homologs under study would also be cleaved by AvrRpt2 to generate fragments similar to those generated upon AtRIN4 cleavage. Co-expression with the effector AvrRpt2-HA in *N. benthamiana* was used to detect AvrRpt2-cleavage of the RIN4 homologs. The YFP-AcV5-RIN4$^{1\Delta RCS1}$ derivatives can be used to track the cleavage fragment, YFP-AcV5-RIN4^{INT}, that is released upon cleavage by AvrRpt2 within the C-NOI. Figure 4a shows that,

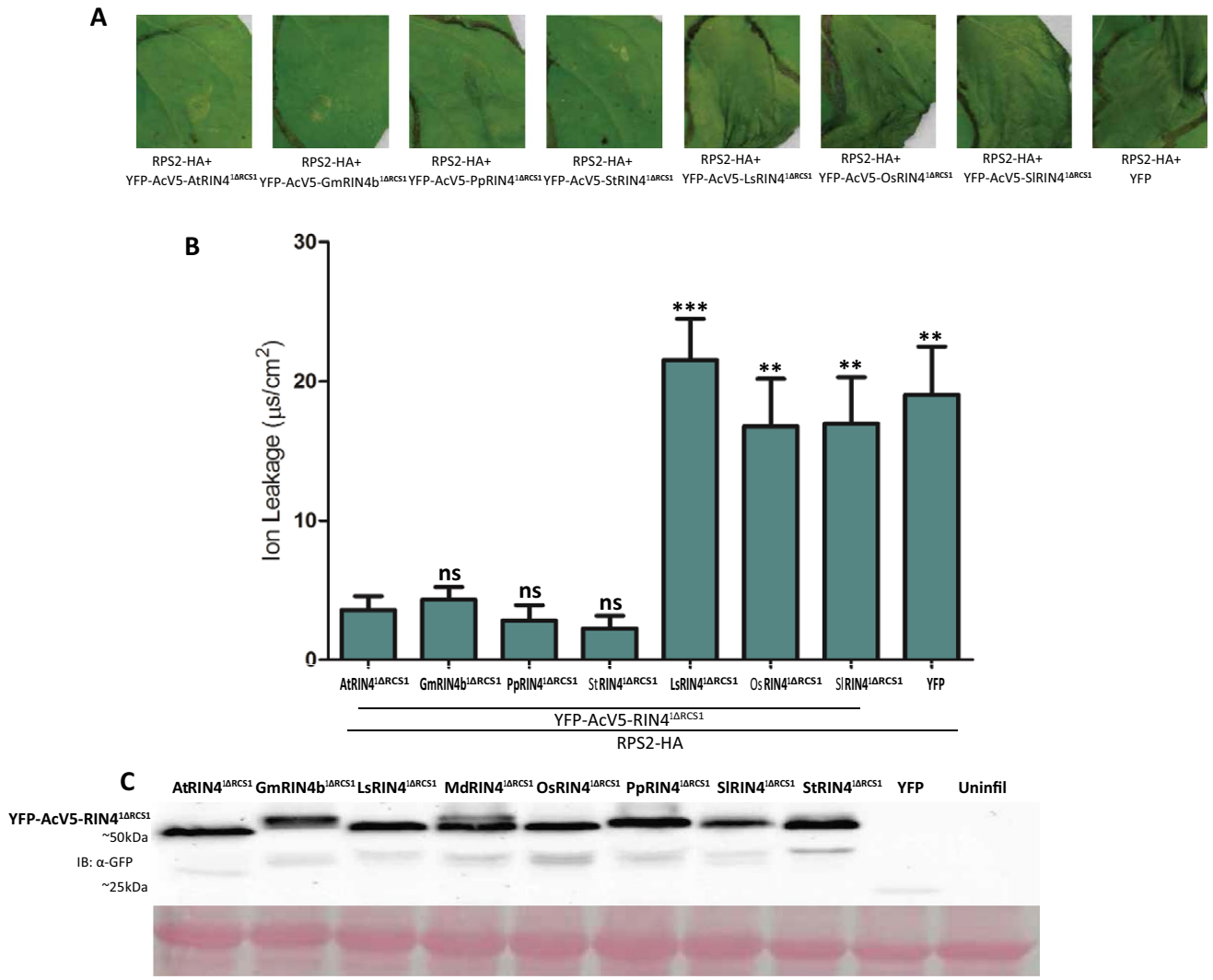

Fig. 3 RIN4 homologs differ in their ability to regulate RPS2. YFP-AcV5-RIN4$^{1\Delta RCS1}$ derivatives (OD_{600} 1.0) and RPS2-HA (OD_{600} 0.1) were transiently expressed in *N. benthamiana.* **A** Macroscopic RPS2-induced cell death was observed at 48 HPI. YFP failed to suppress RPS2-HA (far right panel). Similar to YFP-Acv5-AtRIN4$^{1\Delta RCS1}$, the YFP-Acv5-RIN4$^{1\Delta RCS1}$ versions from soybean, peach and potato also suppressed RPS2-HA. In contrast, the YFP-Acv5-RIN4$^{1\Delta RCS1}$ versions from lettuce, rice and tomato failed to suppress RPS2-HA. **B** Cell death was quantified based on electrolyte leakage. Three leaf discs for each YFP-AcV5-RIN4$^{1\Delta RCS1}$ homolog co-infiltrated with RPS2-HA were collected, immersed in sterile water, and conductivity of the bath solution was measured at 72 HPI. Data were gathered from five independent experiments. Error bars represent SEM. Student's t-test, at 95% confidence limits, was used for comparison with AtRIN4$^{1\Delta RCS1}$ (*ns* not significant; $^{**}P < 0.01$; $^{***}P < 0.001$). **C** Anti-GFP immunoblot conducted on samples from 72 HPI show that YFP-AcV5-RIN4$^{1\Delta RCS1}$ homologs accumulated to a comparable level in *N. benthamiana.* Panels below show ponceau stain for RuBisCO used as loading control. Molecular masses indicate the predicted mobility of the protein(s) of interest

similar to wild-type AtRIN4, cleavage of the YFP-AcV5-RIN4$^{1\Delta RCS1}$ derivatives by AvrRpt2-HA resulted in the relocalization of YFP-AcV5-RIN4^{INT} to the cytosol and the nucleus (Fig. 4a and Supplemental Fig. 6). No change in the localization of the YFP signal was observed upon co-infiltration of the YFP-AcV5-RIN4$^{1\Delta RCS1}$ derivatives with the catalytically inactive mutant, AvrRpt2^{C122A}-HA (Fig. 4a). The localization of the YFP-AcV5-RIN4^{INT} fragments and the intact YFP-AcV5-RIN4$^{1\Delta RCS1}$ derivatives following exposure to AvrRpt2-HA or AvrRpt2^{C122A}-HA, respectively, was confirmed through subcellular fractionation AvrRpt2 cleaves the RCS2 site within each of the RIN4 homologs and generates soluble RIN4^{INT} fragments (Fig. 4b).

AvrRpt2-mediated cleavage of homologs results in the activation of RPS2

After establishing AvrRpt2-mediated cleavage of the RIN4 homologs, we next determined the ability of those homologs

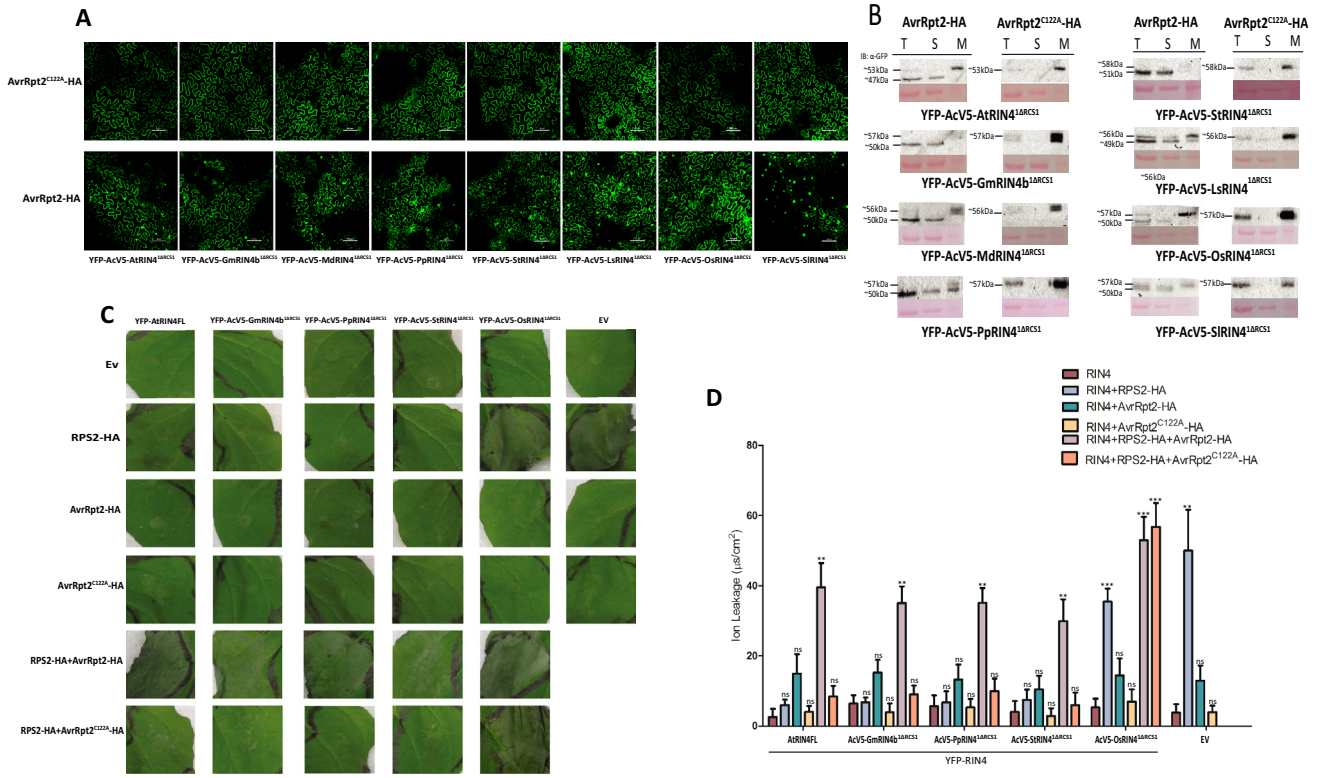

Fig. 4 AvrRpt2-mediated cleavage of the RIN4 homologs generates soluble, internal fragments and activates RPS2. **A** YFP-AcV5-RIN4$^{1\Delta RCS1}$ homologs (OD_{600} 0.6) were co-infiltrated with either AvrRpt2-HA (OD_{600} 0.01) or AvrRpt2^{C122A}-HA (OD_{600} 0.01) in *N. benthamiana* leaves. Localization of the fluorescent signal was observed at 48 HPI using confocal microscopy (Scale bar: 100 μM). Top: Membrane localization of the YFP-AcV5-RIN4$^{1\Delta RCS1}$ derivatives was unaffected by co-expression of AvrRpt2^{C122A}-HA. Bottom: Co-expression of AvrRpt2-HA resulted in the fluorescent signal appearing in the cytosol and nuclei. **B** Anti-GFP immunoblotting was conducted on samples treated as in panel A at 48 HPI that had been fractionated into total (T), soluble (S) and membrane (M) fractions. Right: YFP-AcV5-RIN4$^{1\Delta RCS1}$ derivatives co-infiltrated with AvrRpt2^{C122A}-HA accumulated in the membrane fraction. Left: Co-infiltration of YFP-AcV5-RIN4$^{1\Delta RCS1}$ derivatives resulted in appearance of the YFP-AcV5-RIN4^{INT} fragments in the soluble fraction. Ponceau staining shows RuBisCO as a soluble protein marker. Molecular masses indicate the predicted mobility of the protein(s) of interest. **C** YFP-AcV5-RIN4$^{1\Delta RCS1}$ derivatives (OD_{600} 0.6) were co-expressed in *N. benthamiana* in the indicated combinations with RPS2-HA (OD_{600} 0.09) and/or AvrRpt2-HA or AvrRpt2^{C122A}-HA (OD_{600} 0.01). Macroscopic RPS2-induced cell death was observed at 48 HPI. Similar to YFP-AtRIN4Fl, co-infiltration of YFP-AcV5-RIN4$^{1\Delta RCS1}$ derivatives from soybean, peach and potato with AvrRpt2-HA, but not AvrRpt2^{C122A}-HA, resulted in RPS2 dependent cell death. **D** Cell death was quantified based on electrolyte leakage. Three leaf discs for each combination, as in panel C, were taken, immersed in sterile water, and conductivity of the bath solution was measured at 72 HPI. Data were collected from four independent experiments. Error bars represent SEM. Within a species, all of combinations were compared against the species specific YFP-AcV5-RIN4$^{1\Delta RCS1}$ derivative. Student's t-test, at 95% confidence limits, was used for comparison (ns, not significant; $^{**}P < 0.01$; $^{***}P < 0.001$)

capable of suppressing RPS2, to mediate RPS2 activation in the presence of the effector. Similar to AtRIN4, phosphorylation and ADP-ribosylation of GmRIN4 homologs (particularly GmRIN4a and GmRIN4b) by *P. syringae* effectors, AvrB and AvrRpm1 activates the Rpg1b and Rpg1r R-proteins (Ashfield et al. 2014; Redditt et al. 2019; Selote and Kachroo 2010b). GmRIN4b was also able to restore the activation of RPM1 by AvrB or AvrRPM1 in *rin4 Arabidopsis* plants (Selote and Kachroo 2010b). Similar to the activation of RPS2 upon proteolytic cleavage of AtRIN4, it was recently demonstrated that AvrRpt2-mediated cleavage of SlRIN4 and MdRIN4 also activates the R-proteins SlPtr1 and MdMr5, respectively (Mazo-Molina et al. 2020; Prokchorchik et al. 2020). The C-terminal cleavage fragment of MdRIN4, MdACP3, was both necessary and sufficient for the activation of MR5 (Prokchorchik et al. 2020). These results indicate that effectors from different pathogens elicit NLR-mediated immune responses by targeting RIN4.

To determine if the effector-mediated cleavage of the YFP-AcV5-RIN4$^{1\Delta RCS1}$ homologs resulted in the activation of RPS2, YFP-AcV5-RIN4$^{1\Delta RCS1}$, derivatives of homologs capable of suppressing RPS2 (and the rice derivative as a negative control) were co-infiltrated with RPS2 and/or AvrRpt2. To avoid background cell death caused by high level expression of AvrRpt2, reminiscent of that induced upon high-level expression of AvrB in *N. benthamiana*

(Chung et al. 2011), we used *Agrobacterium* at an OD_{600} of 0.01.

Overexpression of AtRIN4 causes a delay in elimination of the full length protein by AvrRpt2, which in turn inhibits RPS2 activation (Axtell and Staskawicz 2003; Mackey et al. 2003). Similarly, when YFP-AcV5-AtRIN4 was expressed with a high titer of *Agrobacterium* (OD_{600} of 1.0), AvrRpt2 failed to activate RPS2 (data not shown). However, YFP-AtRIN4Fl (full length) expressed at an OD_{600} of 0.6 was able to suppress the ectopic activation of RPS2 and permit activation of RPS2 by AvrRpt2 (Fig. 4c, d). Thus, for this assay, *Agrobacterium* delivering the YFP-AcV5-$RIN4^{1\Delta RCS1}$ homologs was infiltrated at an OD_{600} of 0.6. YFP-AcV5-$RIN4^{1\Delta RCS1}$ homologs from soybean, peach and potato, which were able to suppress ectopic activation of RPS2, also supported the AvrRpt2-mediated activation of RPS2 (Fig. 4c, d). This activity of AvrRpt2 was dependent on its protease activity as $AvrRpt2^{C122A}$ failed to overcome RPS2 suppression by any of the YFP-AcV5-$RIN4^{1\Delta RCS1}$ homologs (Fig. 4c, d). Thus, YFP-AcV5-$RIN4^{1\Delta RCS1}$ homologs from soybean, peach and potato can substitute for AtRIN4 in reconstitution of the AvrRpt2-RPS2 recognition module.

Fragments of RIN4 produced by AvrRpt2 differ in their ability to suppress RPS2

Cleavage of AtRIN4 by AvrRpt2 serves as a trigger for the activation of RPS2 (Axtell and Staskawicz 2003; Mackey et al. 2003). After establishing that AvrRpt2-mediated cleavage of the homologous proteins resulted in the activation of RPS2, the role of the cleavage fragments in the regulation of RPS2 activation was determined. The C-terminal cleavage fragment, $AtRIN4^{CLV3}$, remains tethered at the plasma membrane because of the attached palmitoyl group (Afzal et al. 2011; Chisholm et al. 2005). Similarly, the YFP-$RIN4^{CLV3}$ fragments from the RIN4 homologs also localized at the membrane (Fig. 5a, b). When co-infiltrated in *N. benthamiana,* YFP-$AtRIN4^{CLV3}$ was unable to suppress RPS2 when RPS2 was expressed with *Agrobacterium* at an OD_{600} of 0.075 (Day et al. 2005). Since the YFP-$AtRIN4^{CLV3}$ fragment still localizes at the plasma membrane and contains a mostly intact C-NOI domain, we speculated that it might suppress RPS2 expressed at a lower level. Indeed, YFP-$AtRIN4^{CLV3}$ suppressed RPS2 that was expressed with *Agrobacterium* at an OD_{600} of 0.04 (Fig. 5c, d). Similarly, the YFP-$RIN4^{CLV3}$ fragment of the RIN4 homologs from soybean, peach and potato also suppressed RPS2 (Fig. 5c, d). The YFP-$RIN4^{CLV3}$ fragment from rice, like the YFP-AcV5-$RIN4^{1\Delta RCS1}$ derivative from rice, failed to suppress RPS2 (Fig. 5c, d). Thus, for $RIN4^{1\Delta RCS1}$ homologs able to suppress RPS2, the $RIN4^{CLV3}$ fragments are sufficient to carry out the suppression of RPS2.

We next sought to determine if, similar to the $RIN4^{CLV3}$ fragments, the $RIN4^{INT}$ fragments were able to suppress RPS2. After cleavage, the $AtRIN4^{INT}$ fragment is no longer tethered to the plasma membrane (Afzal et al. 2011; Kim et al. 2005a). As expected, at the YFP-AcV5-$RIN4^{INT}$ fragments of AtRIN4 and the RIN4 homologs localized in the soluble fraction (Fig. 6a, b). $AtRIN4^{11-152}$ is unable to suppress RPS2 expressed with *Agrobacterium* at an OD_{600} of 0.075 (Day et al. 2005). Even when RPS2 was expressed at the lower level, with *Agrobacterium* at an OD_{600} of 0.04, YFP-AcV5-$AtRIN4^{INT}$ was unable to suppress RPS2. Similar to YFP-AcV5-$AtRIN4^{INT}$, the YFP-AcV5-$RIN4^{INT}$ fragments from soybean, peach and potato were also unable to suppress RPS2 (Fig. 6c, d). Taken together, these results indicate that the two cleavage fragments, $RIN4^{INT}$ and $RIN4^{CLV3}$, play contrasting roles in the regulation of RPS2 activation with only the latter able to suppress RPS2.

RPS2 remains at the membrane during ectopic and AvrRpt2-induced activation

After establishing the role of RIN4 homologs and their fragments in regulating RPS2 activity, we next sought to determine the localization of RIN4-suppressed and AvrRpt2-activated RPS2. In the absence of AvrRpt2, RPS2 is localized at the plasma membrane where it interacts with RIN4 (Axtell and Staskawicz 2003; Belkhadir et al. 2004; Mackey et al. 2003). Some R-proteins re-localize upon activation (Burch-Smith et al. 2007; Deslandes et al. 2003). To determine the localization of RPS2 when it is ectopically active (expressed in *N. benthamiana* without RIN4) and when it is activated by AvrRpt2 (expressed in *N. benthamiana* with RIN4 and AvrRpt2), we used the fluorescent-protein tagged, RPS2-YFP-HA, derivative of RPS2. Similar to RPS2-HA, expression of RPS2-YFP-HA with *Agrobacterium* at an OD_{600} of 0.1 resulted in a cell death phenotype and this ectopic activity of RPS2 could be suppressed by the expression of $AtRIN4^{11-211}$ (Supplemental Fig. 7a, b). Thus, the RPS2-YFP-HA was functional.

The ectopic activation of RPS2-YFP-HA (OD_{600} of 0.2) resulted in a cell death phenotype at 42 HPI (Fig. 7a). Ectopically expressed RPS2-YFP-HA predominantly remained localized at the plasma membrane at 40–48 HPI (Fig. 7b). The shape of the epidermal cells remained largely unchanged at these time points (Fig. 7b). By 45 HPI, RPS2-YFP-HA caused significant cell death and even though there was a reduction in the levels of RPS2-YFP-HA, it was still predominately localized at the plasma membrane (Fig. 7b). Notably, RPS-YFP-HA remained membrane localized even in epidermal cells that the bright field imaging indicated were dead or dying (Fig. 7b). As expected, when suppressed by co-expressed $AtRIN4^{11-211}$, no cell death was apparent (Fig. 7a, c), and RPS2-YFP-HA remained localized at

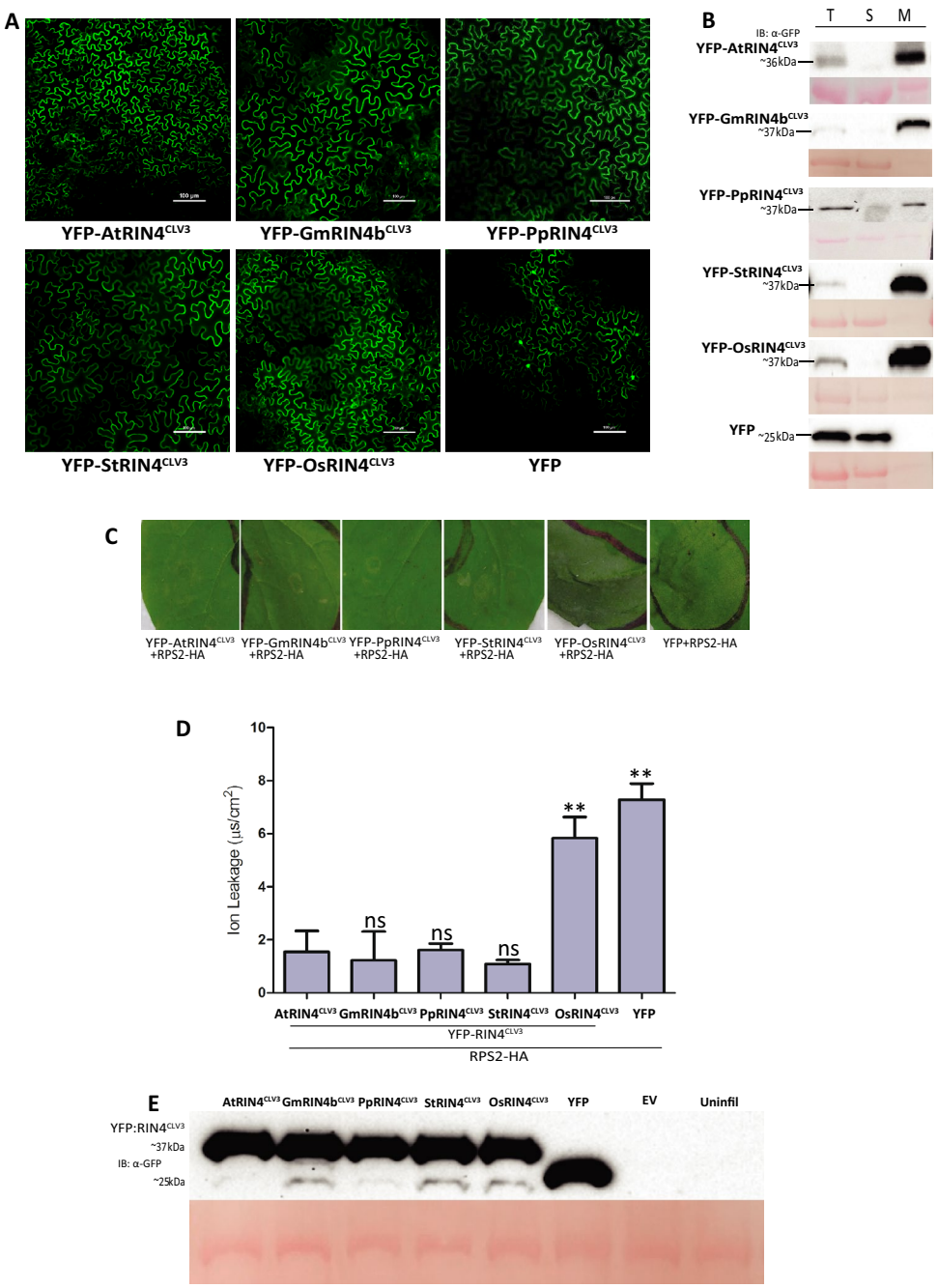

Fig. 5 The YFP-RIN4^{CLV3} fragments are plasma membrane-localized and are capable of suppressing RPS2 in *Nicotiana benthamiana*. **A** YFP-RIN4^{CLV3} fragments (OD_{600} 1.0) were transiently expressed in *N. benthamiana* leaves. Localization of the fluorescent signal was observed at 72 HPI using confocal-microscopy (Scale bar: 100 μM). YFP-RIN4^{CLV3} fragments localized at the membrane, while free YFP protein localized in the cytosol and nuclei. **B** Anti-GFP immunoblotting was conducted on samples treated as in panel A at 72 HPI that had been fractionated into total (T), soluble (S) and membrane (M) fractions. YFP-RIN4^{CLV3} fragments accumulated in the membrane fraction, while the free YFP protein accumulated in the soluble fraction. The panel below shows ponceau stain for RuBisCO used as a soluble protein marker. Molecular masses indicate the predicted mobility of the protein(s) of interest. **C** Co-infiltration of YFP-RIN4^{CLV3} fragments (OD_{600} 1.0) from Arabidopsis, soybean, peach, and potato suppressed macroscopic cell death induced by RPS2-HA (OD_{600} 0.04) at 48 HPI in *N. benthamiana*. Free YFP protein and YFP-OsRIN4^{CLV3} failed to suppress RPS2-HA. **D** Cell death was quantified based on electrolyte leakage. Three leaf discs for the indicated YFP-RIN4^{CLV3} derivatives or free YFP co-infiltrated with RPS2-HA were collected, immersed in sterile water, and conductivity of the bath solution was measured at 72 HPI. Data were collected from four independent experiments. Error bars represent SEM. Student's t-test, at 95% confidence limits, was used for comparison with AtRIN4^{CLV3} (ns, not significant; $^{**}P > 0.01$). **E** Anti-GFP immunoblot conducted on samples from 72 HPI shows that YFP-RIN4^{CLV3} fragments from the different homologs accumulated to comparable levels in *N. benthamiana*. The panel below shows ponceau stain for RuBisCO used as loading control

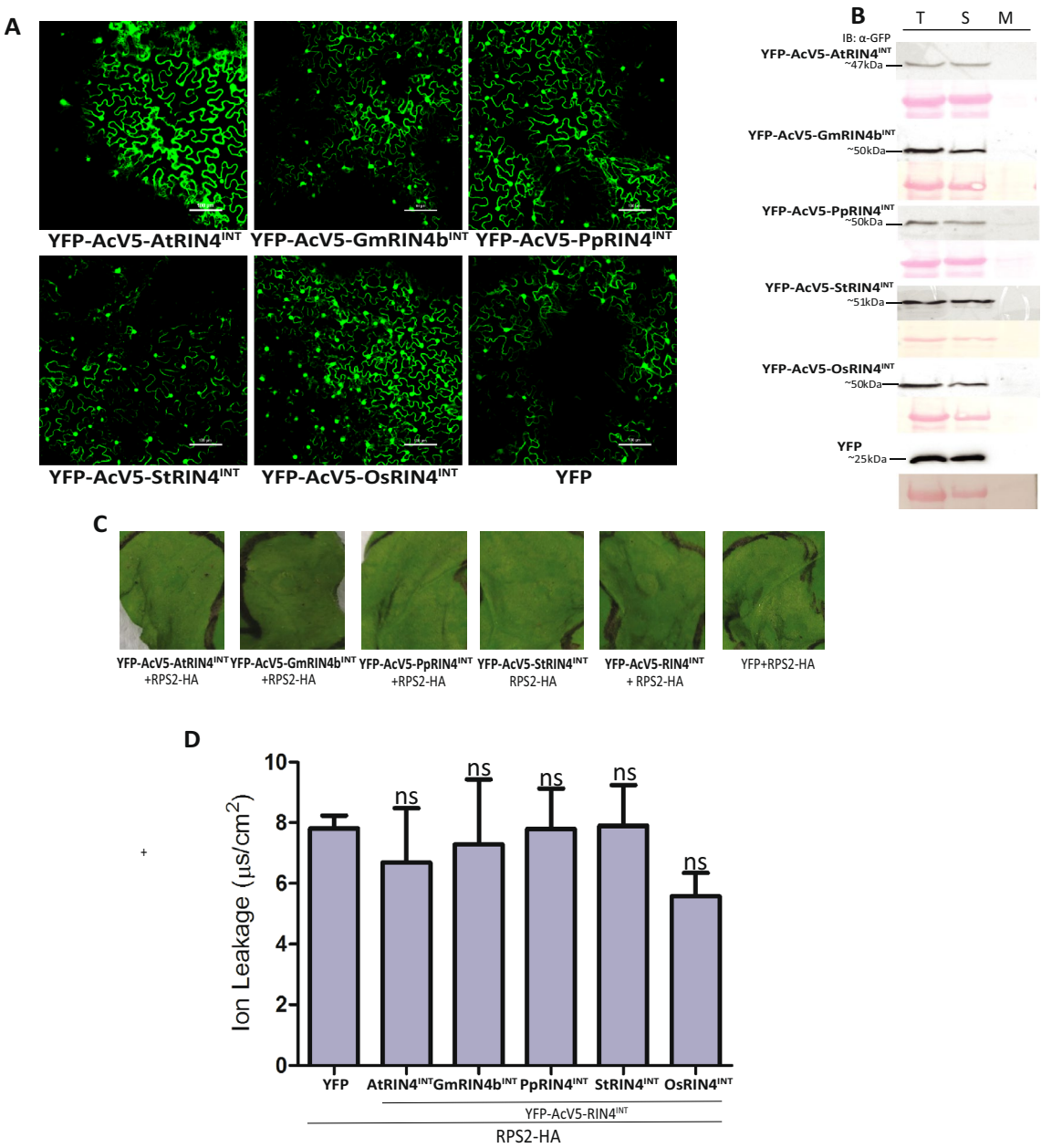

Fig. 6 The YFP-AcV5-RIN4^{INT} fragments are soluble and fail to suppress RPS2 in *Nicotiana benthamiana*. **A** YFP-AcV5-RIN4^{INT} fragments (OD_{600} 1.0) were transiently expressed in *N. benthamiana* plants. Localization of the fluorescent signal was observed at 72 HPI using confocal-microscopy (Scale bar: 100 µM). YFP-AcV5-RIN4^{INT} fragments and the free YFP protein localized in the cytosol and nuclei. **B** Anti-GFP immunoblotting was conducted on samples, as in panel A, from 72 HPI that had been fractionated into total (T), soluble (S) and membrane (M) fractions. YFP-AcV5-RIN4^{INT} fragments and the free YFP protein accumulated in the soluble fraction. The panel below shows ponceau stain for RuBisCO as a soluble protein marker. Molecular masses indicate the predicted mobility of the protein(s) of interest. **C** Macroscopic cell death at 48 HPI of RPS2-HA (OD_{600} 0.04) co-infiltrated with the indicated YFP-AcV5-RIN-4^{INT} fragments or free YFP (OD_{600} 1.0) in *N. benthamiana*. **D** Cell death was quantified based on electrolyte leakage. Three leaf discs for each combination, as in panel C, were taken, immersed in sterile water, and conductivity of the bath solution was measured at 72 HPI. Data were collected from three independent experiments. Error bars represent SEM. Student's *t* test, at 95% confidence limits, was used for comparison with YFP (*ns* not significant)

the membrane (Fig. 7b). We observed similar patterns of membrane localization for ectopically active and RIN4-suppressed RPS2-YFP-HA (OD_{600} of 0.1 and 0.4) at time points when cell death became apparent (Supplemental Fig. 8a, b).

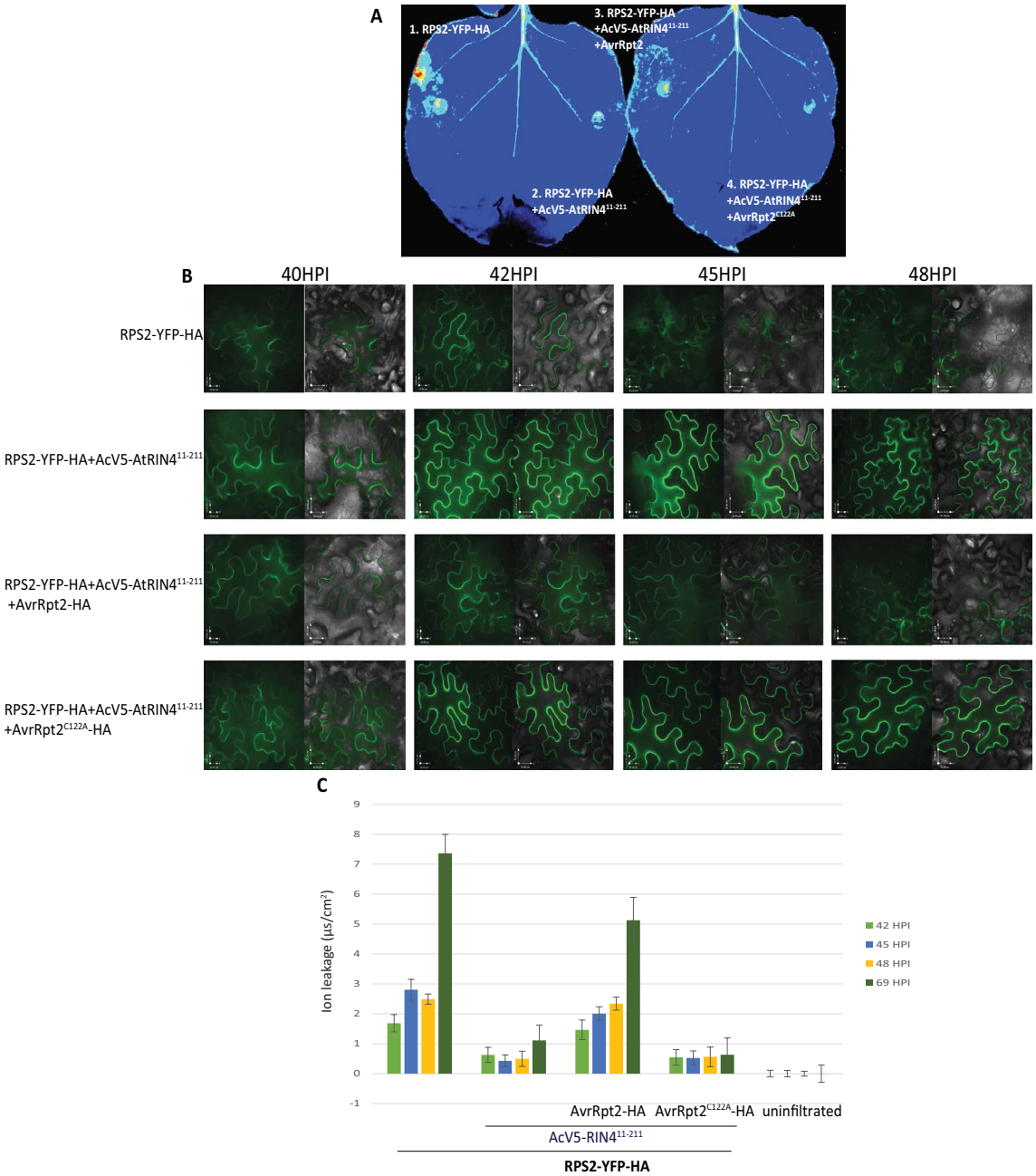

Fig. 7 RPS2 remains membrane-localized during ectopic and AvrRpt2-induced activation. RPS2-YFP-HA (OD_{600} 0.2) and P19 (OD_{600} 0.3) were co-infiltrated with the indicated combinations of AcV5-AtRIN4$^{11-211}$ (OD_{600} 0.6) and AvrRpt2-HA or AvrRpt2^{C122A}-HA (OD_{600} 0.01) in *N. benthamiana* plants. **A** RPS2-induced cell death at 42 HPI in *N. benthamiana* leaves was detected via leaf auto-fluorescence. The signal observed in sections 1 and 3 corresponds to the onset of cell death. **B** Localization of the fluorescent signal was observed at the indicated time points using confocal-microscopy (Scale bar: 15 µM). **C** Cell death was quantified based on electrolyte leakage. Five leaf discs for each combination, as in panel B, were taken at the indicated time points, immersed in sterile water, and conductivity of the bath solution was measured. Data collected from three independent experiments where $n = 15$. Error bars represent SEM

We next examined the localization of RPS2-YFP-HA following its activation by AvrRpt2. When co-infiltrated with AcV5-AtRIN4$^{11-211}$ and AvrRpt2, RPS2-YFP-HA triggered weak cell death at 42 HPI (Fig. 7a, c). Notably, similar to when it is ectopically active, AvrRpt2-activated RPS2-YFP-HA remained detectable and was predominantly present at the plasma membrane at 40–48 HPI (Fig. 7b). Collectively, our results indicate that the plasma membrane localization of RPS2 is unaffected by its suppression/

activation state and that it is thus likely to elicit defense responses, including cell death, at the plasma membrane.

Discussion

AtRIN4 is a member of a highly conserved family of proteins that plays a key role in regulating innate immunity in *Arabidopsis* (Afzal et al. 2013). RIN4 homologs have been reported in plant species ranging from moss to monocots and dicots (Afzal et al. 2013). Conservation of RIN4 homologs across different plant species led to the hypothesis that the encoded proteins might respond to the effectors from plant pathogens in a manner similar to AtRIN4. RIN4 homologs typically contain the general features known to contribute to regulation of immunity, including the NOI domains with embedded AvrRpt2 cleavage sites and a C-terminal acylation motif important for membrane localization (Afzal et al. 2011; Day et al. 2005; Takemoto and Jones 2005). In this study, we have demonstrated that RIN4 homologs from several crop species have predicted C-terminal acylation motifs and, consistent with the functionality of these motifs, are localized at the plasma membrane in *N. benthamiana*. Thus, the function of this membrane targeting strategy appears to be conserved among RIN4 proteins.

Membrane localization of AtRIN4 is required for its ability to prevent ectopic activation of RPS2 (Afzal et al. 2011; Day et al. 2005). We have demonstrated that, while derivatives of all seven RIN4 proteins used in this study localize to the plasma membrane, only those from *Arabidopsis*, soybean, peach, potato and apple are able to suppress RPS2. Since differences in ability of RIN4 homologs to suppress RPS2 are unlikely a result of their expression level or subcellular localization, we speculate that the variability in RPS2 regulation might be due to polymorphisms between RIN4 homologs.

Similar to YFP-AcV5-AtRIN4, AvrRpt2-mediated cleavage of soybean, peach and potato YFP-AcV5-RIN4$^{1\Delta RCS1}$ derivatives resulted in the activation of RPS2. Thus, these RIN4 homologs have the ability to regulate RPS2-mediated immune response against bacterial pathogens carrying the effector AvrRpt2. Proteolysis of the YFP-AcV5-RIN4$^{1\Delta RCS1}$ derivatives by the effector, AvrRpt2, resulted in the generation of RIN4^{INT} and RIN4^{CLV3} fragments. We have demonstrated that these two cleavage fragments differ with respect to regulation of RPS2. The cytosolic RIN4^{INT} fragments are unable to suppress RPS2, while the membrane-tethered RIN4^{CLV3} fragment retain the ability to prevent ectopic activity of RPS2. These observations raise the interesting possibility that RPS2 activation results from the combined activity of the RIN4 cleavage fragments, rather than simply the elimination of full-length RIN4.

Suppression of RPS2 by AtRIN4^{CLV3} and homologous equivalent fragments is in contrast to regulation of Mr5 in apple. Rather than suppressing Mr5, AvrRpt2-induced MdACP3 is required for its activation. And, in the absence of AvrRpt2, MdACP3 is sufficient to activate MR5 (Prokchorchik et al. 2020). Even though RPS2 and MR5 belong to the same CC-NLR class of proteins and recognize AvrRpt2-mediated cleavage of RIN4, they evolved independently (Mazo-Molina et al. 2020; Prokchorchik et al. 2020). It is apparent that the RPS2 and Mr5 NLR-proteins differ in how they are regulated by full-length and AvrRpt2-generated fragments of RIN4. Another NLR-protein, Ptr1 from tomato, has also been shown to respond to the AvrRpt2-mediated cleavage of SlRIN4. It will be of interest to compare the role of AvrRpt2-generated fragments of RIN4 in the regulation of Ptr1 activity.

NLR-proteins localize to a variety of subcellular compartments prior to their activation (Caplan et al. 2008; Gao et al. 2011). In some cases, activation of NLR-proteins results in their re-localization (Burch-Smith et al. 2007; Caplan et al. 2008; Deslandes et al. 2003). In its inactive state, RPS2 is present at the plasma membrane where it interacts with RIN4. Due to its acylation after delivery into a plant cell, AvrRpt2 is also localized at the plasma membrane where it cleaves RIN4 leading to the activation of RPS2 (Coaker et al. 2006). While RPS2 gets activated at the membrane, whether it re-localizes to regulate downstream signaling was unknown. We have demonstrated that RPS2 that has been activated, either ectopically or by AvrRpt2-mediated cleavage of RIN4, remains present at the plasma membrane. Therefore, we conclude that downstream signaling from activated RPS2 does not depend on its re-localization.

Conclusion

Insight into the AvrRpt2-RIN4-RPS2 defense-activation module was gained by comparing the function of AtRIN4 with RIN4 homologs present in a diverse range of plant species. We identified a set of RIN4 homologs, from soybean, peach and potato, that like RIN4 from *Arabidopsis* and apple are able to regulate RPS2-mediated immune responses against AvrRpt2. We speculate that the homologs under study might interact with RPS2-like proteins in their respective host species. Alternatively, these homologs could effectively regulate AtRPS2 introduced into those plant species. We also determined that in addition to their role as negative regulators of basal defenses, the two RIN4 cleavage fragments, RIN4^{INT} and RIN4^{CLV3}, play contrasting roles in the regulation of RPS2. It will be interesting to determine the collective function of these fragments in the AvrRpt2-induced activation of RPS2.

Supplementary Information The online version contains supplementary material available at https://doi.org/10.1007/s00299-021-02771-9.

Author contribution statement AJA and DM designed and conceptualized the study. MA along with JT and AS performed the experiments. MA analyzed the data and drafted the manuscript. Funding was acquired by AJA, DM and MM. Resources for experiments were provided by AJA, SSUH, MM and DM. The project was supervised by AJA, DM and SSUH. The manuscript was reviewed and edited by MA, AJA and DM. All authors read and approved the final manuscript.

Funding Funding support to AJ Afzal was provided by the LUMS Faculty Initiative Fund (FIF) and Start-up grant and by New York University Abu Dhabi and to David Mackey by the National Institute of Health (NIH grant R01GM092772) and Korean Rural Development Administration Next-Generation BioGreen 21 Program (Systemic and Synthetic Agro-biotech Center, PJ01326904). Funding support to Mazin Magzoub was provided by New York University Abu Dhabi.

Declarations

Conflict of interest The authors declare that they have no conflicts of interest.

Ethics declaration N/A.

References

Afzal AJ, da Cunha L, Mackey D (2011) Separable fragments and membrane tethering of *Arabidopsis* RIN4 regulate its suppression of PAMP-triggered immunity. Plant Cell 23:3798–3811

Afzal AJ, Kim JH, Mackey D (2013) The role of NOI-domain containing proteins in plant immune signaling. BMC Genomics 14:327

Ashfield T, Redditt T, Russell A, Kessens R, Rodibaugh N, Galloway L, Kang Q, Podicheti R, Innes RW (2014) Evolutionary relationship of disease resistance genes in soybean and Arabidopsis specific for the Pseudomonas syringae effectors AvrB and AvrRpm1. Plant Physiol 166:235–251

Axtell MJ, Staskawicz BJ (2003) Initiation of RPS2-Specified disease resistance in Arabidopsis is coupled to the AvrRpt2-directed elimination of RIN4. Cell 112:369–377

Belkhadir Y, Nimchuk Z, Hubert DA, Mackey D, Dangl JL (2004) Arabidopsis RIN4 negatively regulates disease resistance mediated by RPS2 and RPM1 downstream or independent of the NDR1 signal modulator and is not required for the virulence functions of bacterial type III effectors AvrRpt2 or AvrRpm1. Plant Cell 16:2822–2835

Bergelson J, Kreitman M, Stahl EA, Tian D (2001) Evolutionary dynamics of plant R-genes. Science 292:2281–2285

Bonardi V, Cherkis K, Nishimura MT, Dangl JL (2012) A new eye on NLR proteins: focused on clarity or diffused by complexity? Curr Opin Immunol 24:41–50

Burch-Smith TM, Schiff M, Caplan JL, Tsao J, Czymmek K, Dinesh-Kumar SP (2007) A novel role for the TIR domain in association with pathogen-derived elicitors. PLoS biology 5:e68

Caplan J, Padmanabhan M, Dinesh-Kumar SP (2008) Plant NB-LRR immune receptors: from recognition to transcriptional reprogramming. Cell Host Microbe 3:126–135

Chiang Y-H, Coaker G (2015) Effector Triggered Immunity: NLR Immune Perception and Downstream Defense Responses. The Arabidopsis Book 13:e0183

Chisholm ST, Dahlbeck D, Krishnamurthy N, Day B, Sjolander K, Staskawicz BJ (2005) Molecular characterization of proteolytic cleavage sites of the Pseudomonas syringae effector AvrRpt2. Proc Natl Acad Sci USA 102:2087–2092

Chisholm ST, Coaker G, Day B, Staskawicz BJ (2006) Host-microbe interactions: shaping the evolution of the plant immune response. Cell 124:803–814

Chung EH, da Cunha L, Wu AJ, Gao Z, Cherkis K, Afzal AJ, Mackey D, Dangl JL (2011) Specific threonine phosphorylation of a host target by two unrelated type III effectors activates a host innate immune receptor in plants. Cell Host Microbe 9:125–136

Coaker G, Zhu G, Ding Z, Van Doren SR, Staskawicz B (2006) Eukaryotic cyclophilin as a molecular switch for effector activation. Mol Microbiol 61:1485–1496

Dangl JL, McDowell JM (2006) Two modes of pathogen recognition by plants. Proc Natl Acad Sci USA 103:8575–8576

Day B, Dahlbeck D, Huang J, Chisholm ST, Li D, Staskawicz BJ (2005) Molecular basis for the RIN4 negative regulation of RPS2 disease resistance. Plant Cell 17:1292–1305

Deslandes L, Olivier J, Peeters N, Feng DX, Khounlotham M, Boucher C, Somssich I, Genin S, Marco Y (2003) Physical interaction between RRS1-R, a protein conferring resistance to bacterial wilt, and PopP2, a type III effector targeted to the plant nucleus. Proc Natl Acad Sci USA 100:8024–8029

Desveaux D, Singer AU, Wu AJ, McNulty BC, Musselwhite L, Nimchuk Z, Sondek J, Dangl JL (2007) Type III effector activation via nucleotide binding, phosphorylation, and host target interaction. PLoS pathogens 3:e48

Dodds PN, Rathjen JP (2010) Plant immunity: towards an integrated view of plant-pathogen interactions. Nat Rev Genet 11:539–548

Eschen-Lippold L, Jiang X, Elmore JM, Mackey D, Shan L, Coaker G, Scheel D, Lee J (2016) Bacterial AvrRpt2-Like cysteine proteases block activation of the *Arabidopsis* mitogen-activated protein kinases, MPK4 and MPK11. Plant Physiol 171:2223–2238

Fan J, Bai P, Ning Y, Wang J, Shi X, Xiong Y, Zhang K, He F, Zhang C, Wang R, Meng X, Zhou J, Wang M, Shirsekar G, Park CH, Bellizzi M, Liu W, Jeon JS, Xia Y, Shan L, Wang GL (2018) The Monocot-Specific Receptor-like Kinase SDS2 Controls Cell Death and Immunity in Rice. Cell host & microbe 23:498–510 e495

Gao Z, Chung EH, Eitas TK, Dangl JL (2011) Plant intracellular innate immune receptor Resistance to Pseudomonas syringae pv. maculicola 1 (RPM1) is activated at, and functions on, the plasma membrane. Proc Natl Acad Sci USA 108:7619–7624

Gill U, Nirmala J, Brueggeman R, Kleinhofs A (2012) Identification, characterization and putative function of HvRin4, a barley homolog of *Arabidopsis* Rin4. Physiol Mol Plant Pathol 80:41–49

Glowacki S, Macioszek VK, Kononowicz AK (2011) R proteins as fundamentals of plant innate immunity. Cell Mol Biol Lett 16:1–24

Hamilton A, Voinnet O, Chappell L, Baulcombe D (2002) Two classes of short interfering RNA in RNA silencing. EMBO J 21:4671–4679

Jeuken MJ, Zhang NW, McHale LK, Pelgrom K, den Boer E, Lindhout P, Michelmore RW, Visser RG, Niks RE (2009) Rin4 causes hybrid necrosis and race-specific resistance in an interspecific lettuce hybrid. Plant Cell 21:3368–3378

Jones JD, Dangl JL (2006) The plant immune system. Nature 444:323–329

Khan M, Subramaniam R, Desveaux D (2016) Of guards, decoys, baits and traps: pathogen perception in plants by type III effector sensors. Curr Opin Microbiol 29:49–55

Kim HS, Desveaux D, Singer AU, Patel P, Sondek J, Dangl JL (2005a) The Pseudomonas syringae effector AvrRpt2 cleaves its C-terminally acylated target, RIN4, from Arabidopsis membranes to block RPM1 activation. Proc Natl Acad Sci USA 102:6496–6501

Kim MG, da Cunha L, McFall AJ, Belkhadir Y, DebRoy S, Dangl JL, Mackey D (2005b) Two Pseudomonas syringae type III effectors inhibit RIN4-regulated basal defense in *Arabidopsis*. Cell 121:749–759

Kim MG, Geng X, Lee SY, Mackey D (2009) The Pseudomonas syringae type III effector AvrRpm1 induces significant defenses by activating the Arabidopsis nucleotide-binding leucine-rich repeat protein RPS2. Plant J 57:645–653

Kumar K, Yadav S, Purayannur S, Verma PK (2013) An alternative approach in Gateway((R)) cloning when the bacterial antibiotic selection cassettes of the entry clone and destination vector are the same. Mol Biotechnol 54:133–140

Lee J, Manning AJ, Wolfgeher D, Jelenska J, Cavanaugh KA, Xu H, Fernandez SM, Michelmore RW, Kron SJ, Greenberg JT (2015) Acetylation of an NB-LRR plant immune-effector complex suppresses immunity. Cell Rep 13:1670–1682

Luo Y, Caldwell KS, Wroblewski T, Wright ME, Michelmore RW (2009) Proteolysis of a negative regulator of innate immunity is dependent on resistance genes in tomato and Nicotiana benthamiana and induced by multiple bacterial effectors. Plant Cell 21:2458–2472

Macho AP, Zipfel C (2015) Targeting of plant pattern recognition receptor-triggered immunity by bacterial type-III secretion system effectors. Curr Opin Microbiol 23:14–22

Mackey D, Holt BF, Wiig A, Dangl JL (2002) RIN4 interacts with pseudomonas syringae Type III effector molecules and is required for RPM1-mediated resistance in *Arabidopsis*. Cell 108:743–754

Mackey D, Belkhadir Y, Alonso JM, Ecker JR, Dangl JL (2003) Arabidopsis RIN4 Is a target of the Type III virulence effector AvrRpt2 and modulates RPS2-mediated resistance. Cell 112:379–389

Mazo-Molina C, Mainiero S, Haefner BJ, Bednarek R, Zhang J, Feder A, Shi K, Strickler SR, Martin GB (2020) Ptr1 evolved convergently with RPS2 and Mr5 to mediate recognition of AvrRpt2 in diverse solanaceous species. Plant J 103:1433–1445

Monteiro F, Nishimura MT (2018) Structural, functional, and genomic diversity of plant NLR proteins: an evolved resource for rational engineering of plant immunity. Annu Rev Phytopathol 56:243–267

Prado GS, Bamogo PKA, de Abreu JAC, Gillet FX, Dos Santos VO, Silva MCM, Brizard JP, Bemquerer MP, Bangratz M, Brugidou C, Sereme D, Grossi-de-Sa MF, Lacombe S (2019) Nicotiana benthamiana is a suitable transient system for high-level expression of an active inhibitor of cotton boll weevil alpha-amylase. BMC Biotechnol 19:15

Prokchorchik M, Choi S, Chung EH, Won K, Dangl JL, Sohn KH (2020) A host target of a bacterial cysteine protease virulence effector plays a key role in convergent evolution of plant innate immune system receptors. New Phytol 225:1327–1342

Redditt TJ, Chung EH, Karimi HZ, Rodibaugh N, Zhang Y, Trinidad JC, Kim JH, Zhou Q, Shen M, Dangl JL, Mackey D, Innes RW (2019) AvrRpm1 functions as an ADP-ribosyl transferase to modify NOI domain-containing proteins, including arabidopsis and soybean RPM1-interacting Protein4. Plant Cell 31:2664–2681

Ren J, Wen L, Gao X, Jin C, Xue Y, Yao X (2008) CSS-Palm 2.0: an updated software for palmitoylation sites prediction. Protein Eng Design Selection 21:639–644

Selote D, Kachroo A (2010a) RIN4-like proteins mediate resistance protein-derived soybean defense against Pseudomonas syringae. Plant Signal Behav 5:1453–1456

Selote D, Kachroo A (2010b) RPG1-B-derived resistance to AvrB-expressing pseudomonas syringae requires RIN4-like proteins in soybean. Plant Physiol 153:1199–1211

Sun X, Greenwood DR, Templeton MD, Libich DS, McGhie TK, Xue B, Yoon M, Cui W, Kirk CA, Jones WT, Uversky VN, Rikkerink EH (2014) The intrinsically disordered structural platform of the plant defence hub protein RPM1-interacting protein 4 provides insights into its mode of action in the host-pathogen interface and evolution of the nitrate-induced domain protein family. FEBS J 281:3955–3979

Tai TH, Dahlbeck D, Clark ET, Gajiwala P, Pasion R, Whalen MC, Stall RE, Staskawicz BJ (1999) Expression of the Bs2 pepper gene confers resistance to bacterial spot disease in tomato. Proc Natl Acad Sci 96:14153–14158

Takemoto D, Jones DA (2005) Membrane release and destabilization of Arabidopsis RIN4 following cleavage by Pseudomonas syringae AvrRpt2. Mol Plant-Microbe Interactions 18:1258–1268

Toruno TY, Shen M, Coaker G, Mackey D (2019) Regulated disorder: posttranslational modifications control the RIN4 Plant immune signaling hub. Mol Plant-Microbe Interactions 32:56–64

Van der Hoorn R (2002) Balancing selection favors guarding resistance proteins. Trends Plant Sci 7:67–71

Weng SL, Kao HJ, Huang CH, Lee TY (2017) MDD-Palm: Identification of protein S-palmitoylation sites with substrate motifs based on maximal dependence decomposition. PloS one 12:e0179529

Whalen MC, Innes RW, Bent AF, Staskawicz BJ (1991) Identification of Pseudomonas syringae pathogens of *Arabidopsis* and a bacterial locus determining avirulence on both *Arabidopsis* and soybean. Plant Cell 3:49–59

Wilton M, Subramaniam R, Elmore J, Felsensteiner C, Coaker G, Desveaux D (2010) The type III effector HopF2 Pto targets *Arabidopsis* RIN4 protein to promote Pseudomonas syringae virulence. Proc Natl Acad Sci 107:2349–2354

Zhou F, Xue Y, Yao X, Xu Y (2006) CSS-Palm: palmitoylation site prediction with a clustering and scoring strategy (CSS). Bioinformatics 22:894–896

Zipfel C (2014) Plant pattern-recognition receptors. Trends Immunol 35:345–351